Polymers and Polymer Composites for Adsorptive Removal of Dyes in Water Treatment

Weiya Huang, Shuhong Wang and Dan Li

List of Abbreviations

AB 25	Acid blue 25
AF	Acid fuchsin
AB	Amido black 10B
AS	Almond shell waste
APT	Attapulgite
BY 28	Basic yellow 28
BF	Basic fuchsin
BV 14	Basic violet 14
CFA	Coal fly ash
CNT	Carbon nanotube
CMC	Carboxymethyl cellulose
mCS/CNT	Magnetic chitosan-decorated carbon nanotube
CR	Congo red
CV	Crystal violet
Bent/CMC-g-P (DMAEMA)	Carboxymethyl cellulose grafted by poly(2-(dimethylamino) ethyl methacrylate) modified bentonite
DB	Direct blue 199
ES	Emeraldine salt
EB	Emeraldine base
EY	Eosin Y
GV	Gentian violet
HA-Am-PAA-B	Humic acid-immobilized amine modified polyacrylamide/ bentonite composite
TRGO/PVA	Hydrothermally reduced graphene oxide/poly (vinyl alcohol)

W. Huang · S. Wang
School of Metallurgy and Chemical Engineering, Jiangxi University of Science and Technology, Ganzhou, China

D. Li (✉)
School of Engineering and Information Technology, Murdoch University, Murdoch, Australia
e-mail: L.Li@murdoch.edu.au

519

hPEI-CE	Hyperbranched polyethyleneimine functionalized cellulose
IC	Indigo carmine
MNPs	Magnetic nanoparticles
MS	Mesoporous silica
MB	Methylene blue
MG	Methylene green
MO	Methyl orange
NR	Neutral red
OVS	Octavinylsilsesquioxane
OR	Oil red O
PAM	Polyacrylamide
PVI	Poly(1-vinyl imidazole)
PSSMA	Poly(4-styrenesulfonic acid-co-maleic acid) sodium
PSSMA/M-rGO	Poly(4-styrenesulfonic acid-co-maleic acid) sodium modified magnetic reduced graphene oxide nanocomposite
Mt	Montmorillonite
Pal	Palygorskite
poly(AN-co-ST)	Poly(acrylonitrile-co-styrene)
PAMAM	Polyamidoamine
PANI	Polyaniline
PANI -FP	Polyaniline-coated filter papers
PANI–MS@Fe_3O_4	Polyaniline functionalized magnetic mesoporous silica composite
PEI	Polyethyleneimine
PmPD	Poly(m-phenylenediamine)
PGA	Poly(γ-glutamic acid)
PVA	Poly (vinyl alcohol)
PV	Proflavine
r-GO-PIL	PVI polymer functionalized reduced graphene oxide
RB5	Reactive black 5
RR228	Reactive red 228
RB	Rhodamine B
RB2	Rose Bengal
TC	Tetracycline
TPE	Tetraphenylethylene
PAmABAmPD	Terpolymer of aniline/m-aminobenzoic acid/ m-phenylenediamine
TCAS	Thiacalix[4]arene tetrasulfonate
β-CD	β-cyclodextrin
20CMC-Bent	20% of CMC in the total amount of CMC + Bent composite
RR2	Reactive red 2
MDI	4,4′-diphenylmethane diisocyanate
TAT	1,3,5-triacryloylhexahydro-1,3,5-triazine

1 Introduction

Natural and synthetic dyes have been commonly used to colour substrates, including food, drugs, cosmetics, paper, leather, plastics and textile products. Synthetic dyes play the dominating role particularly in the fabric and textile industry as compared with natural dyes, which insufficiently meet the industrial demand and therefore are more often used in the food industry [1]. It is estimated that more than 10,000 types of dyes are being used in various industrial applications. According to the literature, more than 8×10^5 tons of synthetic dyes are produced annually worldwide, in which 10–15% is released into natural water environment [2, 3]. Synthetic dyes often exhibit resistance to biodegradation and their persistence in the environment results in pollution, which has become a severe problem worldwide [4]. In particular, many of the synthetic dyes are toxic, carcinogenic and mutagenic. Therefore, dyes in wastewater, even in a small amount, are undesirable and should be properly removed before they enter the environment [5].

According to the applications of dyes, they are classified into groups of acidic, basic, reactive, direct, dispersed, and sulphur dyes; whilst based on the chemical structure of dyes, they are classified as nitro, azo, indigoid, anthraquinone, triarylmethane and nitroso dyes [6]. The most common way is to classify them as anionic (e.g. acid, reactive, and direct dyes), cationic (basic dyes), and nonionic dyes (dispersed dyes), depending on the ionic charge of dye molecules [6]. Cationic dyes were reported with greater toxicity than anionic dyes, because of their easy interaction with negatively charged cell membrane surfaces and entry into cells [5]. The commonly used dyes with their molecular structure, molecular weight, classification and λ_{max} were summarized in Table 4.

In order to remove dyes from wastewater, several biological, chemical and physical methods have been developed, including coagulation, adsorption, membrane separation, precipitation, chemical oxidation, and aerobic or anaerobic treatment [6–8]. Among them, adsorption seems to be the favourite technique because of low cost and diversity of adsorbents, easy operation, environmental and economic sustainability [7, 8]. Various adsorbents have been investigated for dye removal, such as activated carbon, carbon nanotubes, graphene, clay minerals, metal oxides, polymers, non-conventional low-cost adsorbents (e.g. agricultural and industrial waste or by-products), etc. [1, 4, 6, 9–11]. Several parameters, including high adsorption capacity, fast adsorption rate, good selectivity, wide availability, low cost, easy regeneration and feasible reusability, are intensively concerned when designing and selecting a suitable adsorbent to target dye removal. In general, hydrophilic adsorbents are preferable for use, which attract the dye molecules via electrostatic interaction, van der Waals force, π–π interaction, and hydrogen bonding [12].

Recently, polymers and polymer composites have attracted tremendous attention as adsorbents for dye treatments [4, 12–14]. Polymers exhibit a number of excellent properties [13], such as high strength, good flexibility, chemical inertness,

hydrophilic surface chemistry, which are able to act as matrix materials to fabricate polymer composites with inorganics. Their properties can be tuned via functionalization with chemical groups, crosslinking or blending with organic materials which are capable to interact with dye pollutants. Therefore, polymers and polymer composites serve as promising adsorbent materials for high-performance dye removal from water.

The current development of polymers or polymer composites as adsorbents concentrates on the use of nanostructures, such as nanosized particles, which provided great external surface area and exhibited high adsorption to dyes. For example, the nano-sized poly(m-phenylenediamine) (PmPD) exhibited enhanced adsorption capacity, which was calculated by the Langmuir model (387.6 mg/g) towards Orange G (OG), as compared with that of micro-sized PmPD (163.9 mg/g) [15]. However, the nanoparticles might suffer from aggregation, affecting adsorption capacity and kinetics. To improve application potential, polymers and their composites were synthesized in the form of nanofibers, which can be successfully produced by an electrospinning method. These one-dimensional (1D) nanoscale adsorbents, due to their great surface-to-volume ratios, were widely studied for the enhanced properties [16–19]. In addition, porous structures are highly desirable, because they can facilitate the diffusion of dyes into the adsorbents, resulting in fast and efficient adsorption [20]. The porous structure is also favourable to increase the swelling rate of the polymers; however, their mechanic strength would be reduced with increasing porosity. This can be solved by fabricating composite with other inorganic materials, e.g. bentonite [20]. Polymeric adsorbents, in the forms of hydrogels or xerogels which are three-dimensionally crosslinked hydrophilic polymers, were synthesized, functionalized and used as super-adsorbents to remove dyes from aqueous solution, ascribed to their high physicochemical stability and good regeneration property [21–24].

2   Modified or Functionalized Polymers and Polymer Composites

The surface chemistry of adsorbents, such as surface acidity/basicity and points of zero charge, significantly affects the adsorption of dyes. For targeting the removal of anionic dyes, surface properties of adsorbents were modified to minimize negative charge and increase positive charge on surfaces. Since that adsorption takes place on the surfaces of polymer adsorbents, another important factor for consideration is the density of functional groups on surfaces [14, 25]. For example, Qiu et al. synthesized three polystyrene resins with significantly different surface functionality and studied their adsorption performance for an anionic dye Reactive Black 5 dye (RB5), as shown in Fig. 1a [14]. As compared with commercial polymer XAD-4 of a low-degree functionality, NG-8, which was synthesized in the laboratory, had primarily acidic functional groups; and its aminated product MN-8
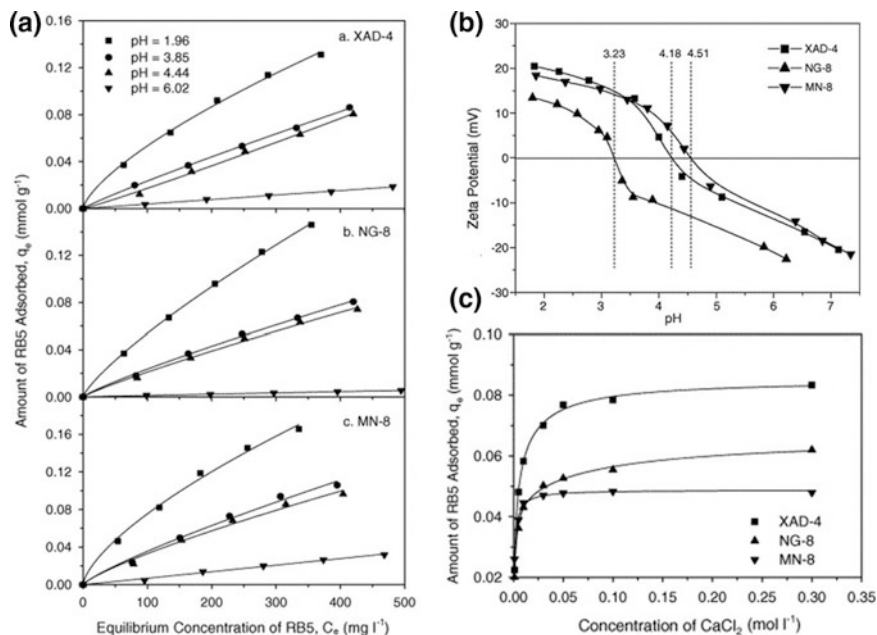
Fig. 1 a Adsorption of RB5 by three different polymers (XAD-4, NG-8, and MN-8) at pH = 1.96, 3.85, 4.44, and 6.02; **b** zeta potentials of XAD-4, NG-8, and MN-8 as a function of solution pH and determined points of zero charge; **c** effect of CaCl$_2$ concentration with initial RB5 concentration of 100 mg/L (reprinted from [14] with permission from Elsevier)

possessed mainly basic amino groups. It was found that XAD-4 exhibited non-polar nature; however moderate polarity was seen for NG-8 and MN-8. Their corresponding point of zero charge was 4.18, 3.23, and 4.51, respectively, as shown in Fig. 1b. The equilibrium adsorption capacity of RB5 for XAD-4, NG-8 and MN-8 was recorded as 115.05, 129.94 and 158.69 mg/g, accordingly, at pH = 1.90 and RB5 equilibrium concentration of 300 mg/L (Table 1). Moreover, the adsorption decreased at high solution pH for all adsorbents. MN-8 was the most effective adsorbent in RB5 removal at all tested pH values; which might probably lie in its increasing basicity caused by the protonation of amine groups and in turn creation of more positive charges on the surface. It was noted that the enhanced adsorption was observed in the presence of CaCl$_2$, as shown in Fig. 1c, possibly ascribed to the neutralization of negative surface charge by Ca^{2+} and RB5-Ca^{2+} pairings [14].

   Some biopolymers, such as chitosan, have a large number of functional groups in their molecules, such as hydroxyl (–OH) and primary amine (–NH$_2$), which can be utilized as functional groups for treatment of dyes due to the electrostatic interaction or hydrogen bonding force [26, 27]. Due to the presence of some groups, such as sulfate (–SO$_3$H) or carboxyl (–COOH), some biopolymers are negatively charged and have potential application for adsorption of cationic dyes [5, 28]. For example, κ-carrageenan is a highly negatively charged natural polysaccharide and was used

Table 1 Dye removal by modified or functionalized polymer composites

Adsorbent	Dye	Adsorption capacity (mg g^{-1})	pH	Temperature (°C)	Initial concentration (mg L^{-1})	References
EDTA-EDA-PAN nanofibers[h]	Methyl orange (MO)	99.15[a]	4	25	5–300	[18]
	Reactive red (RR)	110.0[a]	4	25	5–300	
Ti(IV) functionalized chitosan molecularly imprinted polymer (Ti-CSMIP)	Active brilliant red X-3B	161.1[a]	6.0–7.0	20	/	[27]
Carboxylated functionalized acrylonitrile-styrene co-polymer nanofibers	Basic violet 14 (BV 14)	67.11[a]	6.2	25	1–100	[17]
Silsesquioxane-based tetraphenylethene-linked nanoporous polymers	Rhodamine B (RB)	1666[a]	/	/	/	[34]
	Congo red (CR)	1040[a]				
	Crystal violet (CV)	862[a]				
	Methylene blue (MB)	144[a]				
	Methyl orange (MO)	67[a]				
Mesoporous silica functionalized with polypeptides	Methylene blue (MB)	4.537[b]	/	room temperature	11	[66]
XAD-4[c]	Reactive black 5 (RB5)	115.05[b]/153.73[b]	1.90/6.05[f]	30 ± 0.5	300	[14]
NG-8[d]		129.94[b]	1.90	30 ± 0.5	300	
MN-8[e]		158.69[b]	1.90	30 ± 0.5	300	
Crosslinked chitosan with TAT[g]	Acid orange 7	858.28[b]	5.0	40	/	[31]

(continued)

Table 1 (continued)

Adsorbent	Dye	Adsorption capacity (mg g^{-1})	pH	Temperature (°C)	Initial concentration (mg L^{-1})	References
	Acid red 88	640.61^b	6.0	40	/	
Hydrothermally reduced graphene oxide/poly (vinyl alcohol) (TRGO/PVA) aerogels	Neutral red (NR)	306.2^a	7	30	/	[12]
	Indigo carmine (IC)	250.0^a	2	30	/	
Functional poly(m-phenylenediamine) nanoparticles	Orange G (OG)	387.6^a	/	30	/	[15]
β-cyclodextrin functionalized poly (styrene-alt-maleic anhydride)	Basic fuchsin (BF)	295^b	6.5 ± 0.1	25	20–350	[32]
	Methylene blue (MB)	528^b	6.5 ± 0.1	25	20–350	
Poly(1-vinylimidazole) (PVI) -modified graphene sheets	Methyl blue	1910^a	/	room temperature	100–700	[36]
Cellulose functionalized with hyperbranched Polyethylenimine	Congo red (CR)	2107^a/2100^b	5.0	25	100–1000	[25]
	Basic yellow 28 (BY28)	1865^a/1860^b	9.0	25	100–1000	

^{a}Maximum adsorption capacities calculated by Langmuir model

^{b}Equilibrium adsorption capacity

^{c}A representative St-DVB resin developed by Rohm & Haas, displays an excellent adsorptive affinity for small organic compounds (e.g., phenols), was purchased from Rohm & Haas (Philadelphia, PA)

^{d}Was synthesized using the Friedel-Crafts reaction through self-crosslinking of a chloromethylated copolymer of St-DVB

^{e}Was obtained by aminating swollen NG-8 using 40% dimethylamine solution at 45 °C for 10 h

^{f}pH = 6.05 solution with 0.01 mol l^{-1} CaCl$_2$

^{g}Chitosan crosslinked with 1,3,5-triacryloylhexahydro-1,3,5-triazine (TAT)

^{h}Ethylenediaminetetraacetic acid (EDTA) and ethylenediamine (EDA) crosslinker modified electrospun polyacrylonitrile (PAN) nanofibers

to modify carbon nanotubes to improve the adsorption performance for cationic dye methylene blue (MB) [5]. The magnetite nanoparticles decorated with poly (γ-glutamic acid) (PGA), which is an anionic polypeptide with α-carboxyl groups and synthesized by Bacillus species in a fermentation process, had the Langmuir maximum adsorption capacity of 78.67 mg/g for MB [28].

To enhance their adsorption performance for dye removal, it is an effective way by introducing new functional groups or increasing the density of surface functionality. For example, Wang et al. chemically modified biopolymer chitosan via carboxymethylation, which introduced different amounts of active –OH, –COOH, and –NH$_2$ groups onto the chitosan by controlling the degree of substitution. The resulting N, O-carboxymethyl chitosan showed enhanced adsorption capacity to remove cationic dye MB, with the Langmuir maximum adsorption capacity of 351 mg/g [29]. It is also a good method to fabricate bifunctional materials, which show applications in not only dye decolourization, but also other areas, such as heavy metal ion removal and bacterial capturing [30, 31]. Functional groups, such as amine, can be protonated to be positively charged and adsorb negatively charged dye molecules via electrostatic attraction. For example, the cellulose functionalized with quaternary ammonium groups had an enhanced adsorption of 190 mg/g at pH = 3 for reactive red 228 (RR228), due to the electrostatic attraction (cellulose-R-N$^+$ (C$_2$H$_5$)$_3$···SO$_3^-$) between the positive quaternary ammonium group and SO$_3$H group from negatively charged dye molecules RR228 [3]. Other functional groups, e.g. carboxylic, can improve the polarity of adsorbent to enhance its sorption affinity to cationic dyes [17, 32]. For example, the carboxylated poly (acrylonitrile-co-styrene) nanofiber showed the Langmuir-derived maximum dye adsorption capacity, 67.11 mg/g, when removing basic violet 14 dye (BV 14) (as shown in Table 1). Its adsorption equilibrium was achieved within 30 min and the dye adsorption followed the pseudo-second-order model, suggesting chemisorption [17]. In addition to carboxyl functional groups, the internal hydrophobic cavity in the functional molecule β-cyclodextrin (β-CD), which is a torus-shaped cyclic oligosaccharide made up of seven α-1,4-linked-D-glucopyranose units, formed inclusion complexes with dye organic molecules through host-guest interactions. As a result, the β-CD functionalized poly (styrene-alt-maleic anhydride) adsorbent showed a high equilibrium adsorption quantity of 272.56 and 366.35 mg/g for basic fuchsin (BF) and MB (at pH = 6.5, and initial BF and MB concentration of 95.7 and 93.6 mg/L) (Table 1), respectively; which was one magnitude greater than that of the unfunctionalized adsorbent [32]. In addition, the adsorption capacities increased with increasing initial dyes concentrations from 20 to 350 mg/L, and their Langmuir maximum adsorption capacity for BF and MB reached 298.5 and 531.9 mg/g, respectively [32].

The fabrication of polymers consisting of different organic segments can improve their physical and chemical properties [4, 22]. It would endow new properties to the resulting polymeric materials for dye decolourization applications [17, 33]. Chitosan is a copolymer of D-glucosamine and N-acetyl-D-glucosamine units with a large number of –OH and –NH$_2$ groups; it is prepared by the N-deacetylation of chitin in an aqueous alkaline solution [4]. These functional

groups on chitosan chains work as sites for electrostatic interaction and coordination in dye adsorptive removal. However, the disadvantage of ready dissolution in an acidic medium makes the phase separation very difficult, thus limiting its application for dye removal. Chemical modification by crosslinking, grafting and/or other methods can improve its stability in acidic solution and enhance its mechanical strength [4]. After introducing a hexahydrotriazine ring into the crosslinked structure of chitosan with 1,3,5-triacryloylhexahydro-1,3,5-triazine (TAT), the crosslinked chitosan showed the promising adsorption of 858.28 mg/g towards CI Acid Orange 7 at pH 5.0, while that of 640.61 mg/g to Acid Red 88 at pH 6.0, as shown in Table 1 [31]. Besides, the flexibility of the structure of the modified polymer materials might have some certain effect on the adsorption process [31]. Poly(acrylonitrile-co-styrene) (poly(AN-co-ST)), as an important random copolymer of acrylonitrile and styrene, exhibits high resistance to heat, chemicals and oil, accompanied with other features, e.g. high rigidity and superior transparency [17]. The carboxylated functionalized poly(AN-co-ST) nanofibers exhibited a good adsorption capacity to BV 14, with the maximum capacity of 67.11 mg/g, as shown in Table 1. Liu et al. fabricated a series of hybrid polymers after the Friedel–Crafts reaction of tetraphenylethylene (TPE) and octavinylsilsesquioxane (OVS) (Fig. 2a, b) [34]. In addition to the high luminescence properties ascribed to TPE, the resulting silsesquioxane based TPE-bridged polymers had found adsorption use in gas, dye and metal ion detection. Particularly, the adsorption capacity of hybrid polymer for cationic dye rhodamine B (RB), anionic dye congo red (CR) and crystal violet (CV) was 1666, 1042 and 862 mg/g, respectively, as shown in Table 1. The adsorption process was mainly governed by size-selective mechanism ascribed to the unique bimodal pore structure in the hybrid polymers with micropores centring at $\sim$ 1.4 nm and mesopores centring at $\sim$4.5 nm, as well as the high surface area of up to 1910 cm^2/g [34]. Zhu et al. modified cellulose with cationic hyperbranched polyethyleneimine (hPEI) via forming Schiff base structure between the amino groups of hPEI and the aldehyde groups on the chemically oxidized cellulose surface (Fig. 2c, d). Because of a large number of amino groups, the resulting functionalized hPEI-CE copolymers displayed the high Langmuir-derived adsorption capacity of 2107 mg/g to anionic dye CR at pH 5.0 and that of 1865 mg/g to cationic basic yellow 28 (BY28) at pH 9.0, since the pH$_{pzc}$ of the copolymer was recorded at pH 8.6 [25].

Recently, the combination of organic and inorganic materials has become an important strategy to modify properties of adsorbents. The resulting adsorbents may not only take advantage of the characteristic of each material, but also improve adsorption performance [27, 35]. Several inorganic compounds or materials, such as mesoporous silica or carbon, carbon nanotubes, graphene, clay, fly ash, metal oxides, and inorganic salts, etc, have been widely used to fabricate inorganic-organic materials as adsorbents. Among them, graphene has drawn significant research interest [12, 36], which can form covalent bonds with a polymer, e.g. as shown in Fig. 3a, by utilizing a diazonium addition reaction and the subsequent grafting of poly(1-vinyl imidazole) (PVI) onto the graphene via a quaternarization reaction. The resulting PVI polymer functionalized reduced graphene
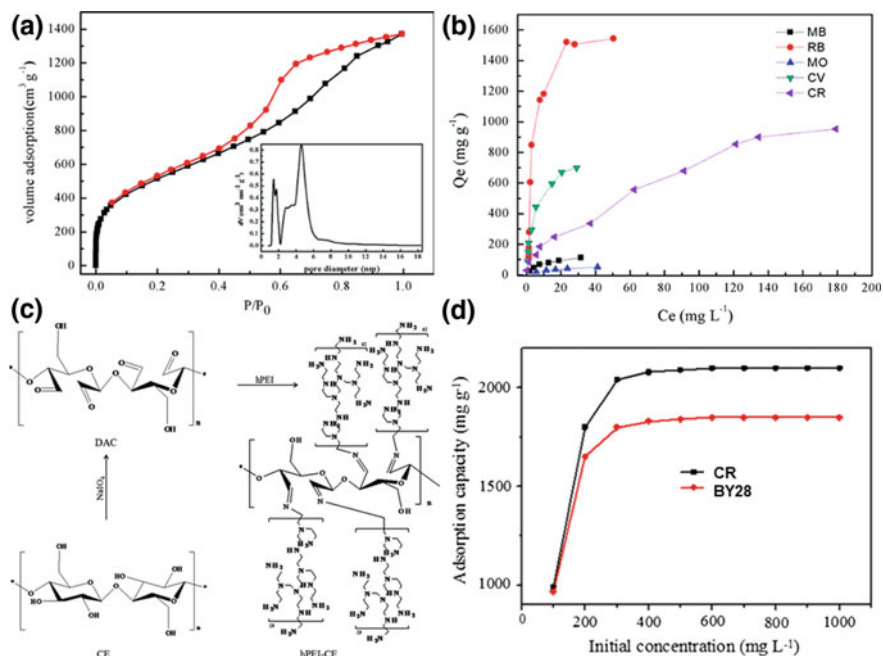
Fig. 2 a N$_2$ adsorption-desorption isotherm (inset:pore-size distribution) and **b** equilibrium adsorption capacity of silsesquioxane based TPE-bridged polymers (reproduced from [34] with permission of The Royal Society of Chemistry); **c** synthesis of cationic hyperbranched polyethyleneimine (hPEI) functionalized cellulose (hPEI-CE) and **d** initial concentration on the adsorption capacity of hPEI-CE for CR and BY28 (reproduced from [25])

oxide (r-GO-PIL) displayed enhanced adsorption efficient towards anionic dyes methyl blue as compared to the unmodified graphene (r-GO), as shown in Fig. 3b. The adsorption equilibrium was almost reached after 1120 min, as shown in Fig. 3c. The adsorption process fitted well with the Langmuir isotherm model and the maximum adsorption capacity was 1910 mg/g; such highly effective absorption was explained by the van der Waals forces and electrostatic interactions between r-GO-PIL and dye [36]. Xiao and co-workers fabricated hydrothermally reduced graphene oxide/poly (vinyl alcohol) (TRGO/PVA) in the form of aerogels via an in situ hydrothermal reduction followed by direct sol-aerogel transformation strategy (Fig. 4a–d). The resulting materials showed an attractive adsorption of various cationic, anionic and nonionic dyes. Their Langmuir-derived maximum adsorption capacity for cationic neutral red (NR) and anionic indigo carmine (IC) dye was 306.2 and 250.0 mg/g (Table 1), respectively (Fig. 4e). Noticeably, other common cationic, anionic or nonionic dyes were also able to be removed by the TRGO/PVA aerogel (Fig. 4f). This attractive adsorption capacity was mostly due to the $\pi - \pi$ interactions between aromatic or heterocyclic structures of dyes and graphene sheets; whilst the additional electrostatic attraction contributes to
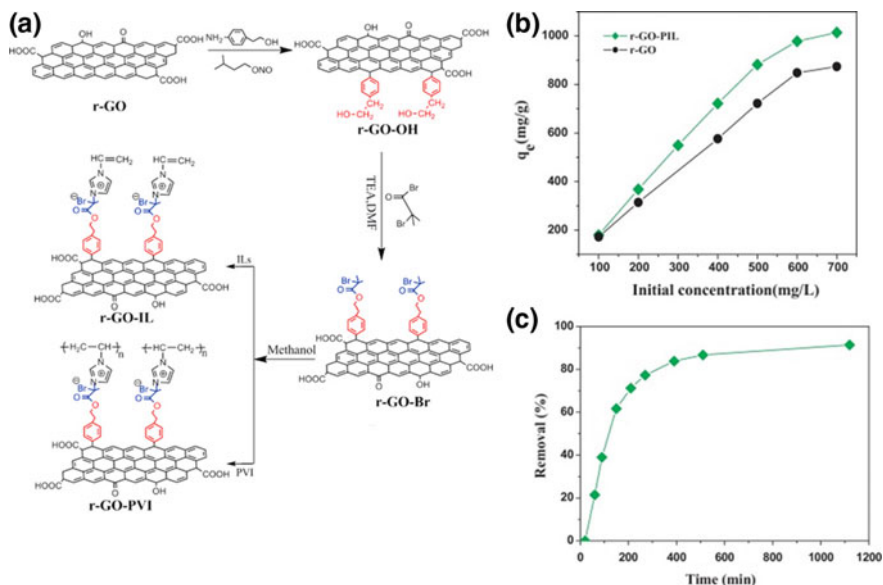
Fig. 3 **a** Grafting of poly(1-vinyl imidazole) onto the surface of the chemically reduced graphene oxide; **b** adsorption capacity of r-GO and r-GO-PIL for the methyl blue at room temperature; **c** Removal of MB by r-GO-PIL as a function of time (initial concentration of dye: 350 mg/L, solution volume: 30 mL, amount of r-GO-PIL: 5 mg) (reprinted from [36] with permission from Elsevier)
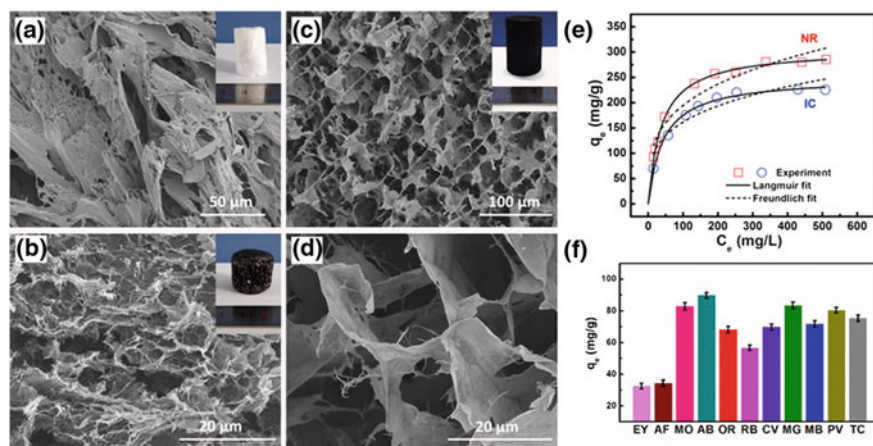

Fig. 4 SEM images of poly (vinyl alcohol) (PVA) **a**, TRGO **b**, and TRGO/PVA (0.5 wt%/1.0 wt %) (**c**: low magnification, **d**: high magnification) aerogels (insets: optical photographs of aerogels); **e** adsorption isotherms using TRGO/PVA (0.5 wt%/1.0 wt%) aerogel fitted by the Langmuir and Freundlich models; **f** adsorption of anionic dyes, eosin Y(EY), acid fuchsin (AF), methyl orange (MO) and amido black 10B (AB) (at pH = 2), as well as the adsorption of nonionic dye, oil red O (OR), cationic dyes, RB, CV, methylene green (MG) and MB, and aromatic drugs, proflavine (PV) and tetracycline (TC) (at pH = 7) (reprinted from [12] with permission from Elsevier)

higher adsorption of cationic dye NR than anionic dye IC [12]. More progress on the development of inorganic-organic adsorbents has been reviewed in the following sections.

3 Polyaniline and Its Composites

Polyaniline (PANI) is one of the amine-containing conjugated polymers, which has been extensively investigated during the last two decades. Many merits have been realized in related to its properties, such as good environmental stability, low-cost monomers for synthesis, high conductivity, instinct redox property, air and moisture stability, water insolubility and flexibility [37–39]. It has been found applications for different purposes, including anti-corrosion coating, batteries and sensors, supercapacitor and optoelectronic devices [15, 37, 39, 40]. Especially, PANI has incredible potential in treating dye-polluted water, because of the presence of amine and imine functional groups, which can act as the chelating and adsorbing sites through electrostatic interaction or hydrogen bond [8, 24]. When these nitrogen-containing functional groups are protonated, PANI is present in its emeraldine salt (ES) state; whilst those are deprotonated, PANI exhibits in its form of emeraldine base (EB). This conversion can be easily achieved by the treatment using acid or base [41]. It is notable that the deprotonated PANI-EB favours the selective adsorption of cationic dyes; whilst the PANI-ES preferentially adsorbs anionic dyes due to the electrostatic interactions. This was supported by Majumdar's research [42], that the polyaniline-coated filter papers in both PANI (ES)-FP and PANI (EB)-FP forms were synthesized to remove seven different anionic dyes and cationic dyes. The Langmuir adsorption capacity of Eosin yellow (EY) (as an anionic model dye) on PANI (ES)-FP was 4.3 mg/g and that of MB (as a cationic model dye) on PANI (EB)-FP was 1.3 mg/g at neutral pH. Figure 5a schematically shows the adsorption of dyes by PANI (ES)-FP and PANI (EB)-FP.

It is noted that the use of PANI powders as adsorbent could be limited by its surface area [43]. Research interest was attracted at the fabrication of PANI into various nanostructures, i.e. nanoparticles and nanotubes [38, 44], or its composite with the incorporation of nanosized inorganics [8, 40, 45]. Various inorganic materials, such as mesoporous silica, carbon nanotubes, nanosized metal or metal oxide (e.g. Ag, γ- Al_2O_3, MgO, and ZrO_2), as well as metal salts (e.g. cupric chloride, α-zirconium phosphate, et al.), have been explored; the summary of those works is shown in Table 2 [8, 37, 38, 41, 43, 45–47]. For example, PANI/γ- Al_2O_3 nanocomposite was fabricated by in situ polymerization of aniline in the presence of γ- Al_2O_3 nanoparticles, as shown in Fig. 5b. The PANI/γ- Al_2O_3 nanocomposite showed a high adsorption capacity of 1000 mg/g for cationic dye Direct blue 199 (DB) at pH 2, calculated by the Langmuir isotherm model. The adsorption process was proceeded via electrostatic attraction between the protonated ammonia groups in PANI ($R-NH_3^+$) and sulfonic groups from anionic dye ions ($D-SO_3^-$), in the form of ($R-NH_3 \cdots O_3S-D$) [8].
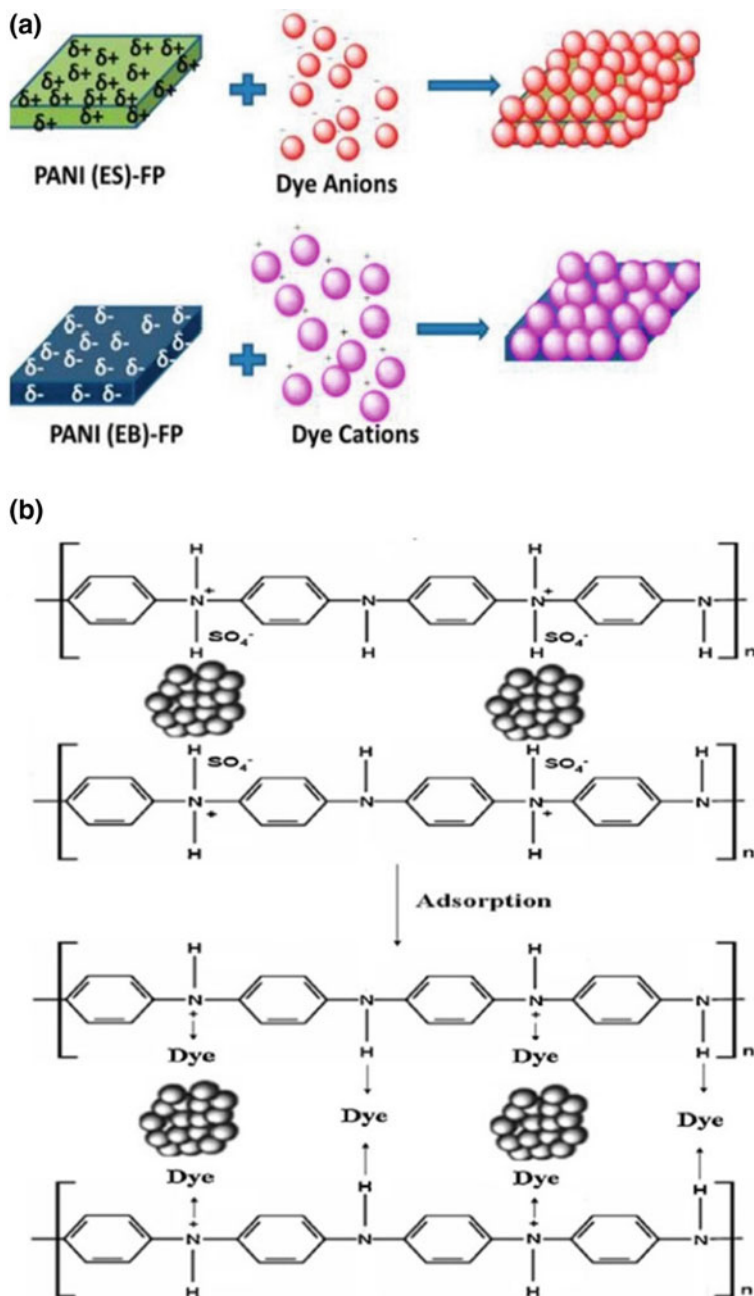
Fig. 5 a Schematic of adsorption of anionic and cationic dyes by PANI (ES)-FP and PANI (EB)-FP; **b** adsorption of anionic dyes by PANI/γ- Al₂O₃ nanocomposite (modified & reprinted with permission from [42, 8])

Table 2 Dye removal by polyaniline (PANI) composites

Adsorbent	Dye	Adsorption capacity (mg g^{-1})	pH	Temperature (°C)	Initial concentration (mg L^{-1})	References
PANI/zirconium oxide	Methylene blue (MB)	77.51[a]	/	26 ± 1	10–40	[37]
PANI/MgO	Reactive orange 16 (RO)	558.4[a]	7	30	50–250	[43]
PANI/γ- Al$_2$O$_3$	Reactive red 194	71.9[a]	2	25	/	[8]
	Acid blue 62	222.2[a]	2	25	/	
	Direct blue 199	1000[a]	2	25	/	
PANI doped with 8% CuCl$_2$	Cibacron navy P-2R-01	99.83%[b]	6	25	60	[47]
PANI/Ag nanocomposite	Brilliant green (BG)	23.66[a]	/	30	/	[45]
PANI/α-zirconium phosphate	Methyl orange (MO)	377.46[a]	4	/	/	[38]
PANI nanotube	Methyl orange (MO)	254.15[a]	4	/	/	[38]
Carbon nanotube/PANI	Malachite green (MG)	13.95%/88%[b]	7	20	16	[41]
Folic Acid-PANI	Eosin yellow (EY)	247.5[a]	3	25	100–230	[24]
	Eosin yellow (EY)	239[e]	3	25	200	
	Rose Bengal (RB2)	206[e]	3	25	200	
	Methyl orange (MO)	173[e]	3	25	200	

(continued)

Table 2 (continued)

Adsorbent	Dye	Adsorption capacity (mg g^{-1})	pH	Temperature (°C)	Initial concentration (mg L^{-1})	References
Fe$_3$O$_4$@AmABAmPD-TCAS[c]	Methylene blue (MB)	31.64[a]	8	30	5–50	[33]
	Malachite green (MG)	29.07[a]	8	30	5–50	
PANI-MS@Fe$_3$O$_4$[d]	Methyl orange (MO)	55.74[a]	4	0	4–32	[48]
PANI emeraldine salt (ES)-coated	Eosin yellow (EY)	4.26[a]	7	/	1–25	[42]
filter paper	Methylene blue (MB)	1.26[a]	7	/	1–25	

[a]Maximum adsorption capacity calculated by Langmuir isotherm model
[b]Removal rate %
[c]The adsorbent is composed of a Fe$_3$O$_4$ core and polyaniline–aminobenzoic acid–phenylenediamine terpolymer shell functionalized with thiacalix(4)arene tetrasulfonate as the internal dopant
[d]Polyaniline functionalized magnetic mesoporous silica iron oxide (MS@Fe3O4) nanoparticles
[e]Equilibrium adsorption capacity

A synergistic effect of PANI and inorganic materials was seen on improving the adsorptive removal of dyes from the literature [37, 40, 43]. For example, the carbon nanotube (CNT)/PANI composites fabricated by Zeng et al. had an equilibrium adsorption capacity of 13.95 mg/g for cationic dye malachite green (MG) at an initial MG concentration of 16 mg/L, which was 15% higher than that of neat PANI. This was probably due to the strong interaction of CNT-PANI, as well as its high porosity and large surface area [41]. Wang and co-workers synthesized PANI and α-zirconium phosphate composite (PANI/α-ZrP) via in situ oxidative polymerization reaction. The resulting PANI/α-ZrP exhibited BET surface area of 30.40 m^2/g, showing plate-like α-ZrP structures decorated by PANI thin layer of small and uniform fibrillar nanostructure (Fig. 6b); this differed from the structure of PANI nanotube (Fig. 6a). Thanks to this unique structure, the PANI/α-ZrP composites showed the Langmuir-derived maximum methyl orange (MO) adsorption of 377.46 mg/g, which was greater than that of PANI nanotubes (254.15 mg/g), as shown in Fig. 6c. In the kinetic study (Fig. 6d), the fast adsorption in first 60 min was probably ascribed to the electrostatic interactions between sorption sites of PANI/α-ZrP, i.e. amine and imine functional groups,
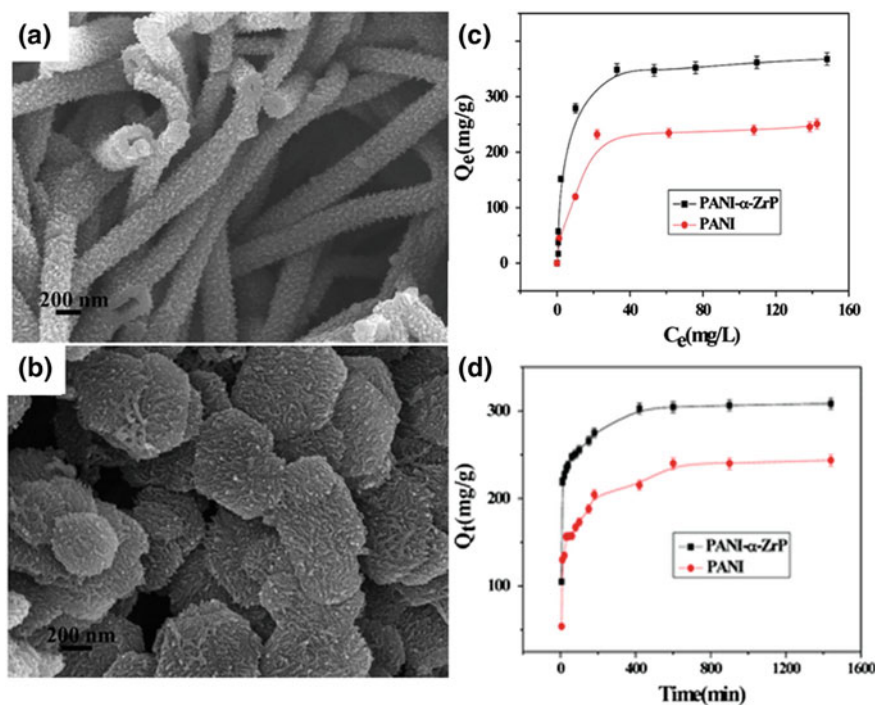
Fig. 6 SEM images of **a** PANI, **b** PANI/α-ZrP (α-ZrP/aniline mol ratio = 1:30); **c** adsorption isotherms of MO on PANI nanotubes and PANI/α-ZrP nanocomposites; **d** adsorption kinetics curves for the adsorption of MO with initial concentration of 100.0 mg/L by PANI nanotubes and PANI/α-ZrP nanocomposites (reprinted with permission from [38])

and MO molecule; after that, the adsorption process slowed down and reached equilibrium [38].

Organic functional materials, such as folic acid, aminobenzoic acid, phenylenediamine, etc., and other materials, e.g. low-cost filter paper, have been used to improve the properties of PANI for dye-containing water purification, as shown in Table 2 [24, 33, 42]. For example, Das et al. fabricated a novel porous folic acid/PANI hydrogel, in which folic acid was used as a cross-linker to PANI. The as-synthesized folic acid/PANI hydrogel exhibited high specific surface area with 3D interconnected pores. The folic acid/PANI xerogels were found efficient in removing anionic dyes, such as EY, Rose Bengal (RB2), MO, ascribed to the electrostatic attraction between anionic dyes and positively charged PANI, which was presented in emeraldine salt (ES) state [24]. Moreover, magnetic nanoparticles, such as Fe_3O_4, were introduced to PANI composites for efficient magnetic separation and reuse [33, 48]; this has been covered in the following section.

4 Magnetic Polymer Composites

The development of magnetic polymer composites is of importance for recycling and reusing in practical application. The magnetic separation offers the ability to recover and reuse the suspended adsorbents after multiple cycles of adsorption, which is of great significance for sustainable process management. In particular, the magnetic separation is believed to be more efficient than conventional centrifugation and filtration, which might be subject to the risk of blockage of filters and loss of adsorbents [5, 49].

In the past decades, the adsorbents combined with magnetic nanoparticles (MNPs) have attracted great research interest, ascribed to their good adsorption capacity, high adsorption rate and convenient recycling of solids by employing an external magnetic field. Fe_3O_4 MNPs are most commonly used as magnetic particles due to their unique property such as low toxicity, biocompatibility and easy handling of magnetic separation [5, 50, 51]. Fe_3O_4 MNPs can be synthesized by precipitation in a fine mixture of Fe(II) and Fe(III) solution with ammonium hydroxide under nitrogen atmosphere [28], or via a solvothermal route under heating [26]. However, the practical application of bare Fe_3O_4 MNPs has seen several limitations, such as the leaching of iron in strong acid solution and a high tendency to aggregate [28]. Therefore, an effective surface coating of Fe_3O_4 MNPs with appropriate coating materials, such as inorganic silica or polymer is necessary to enhance the stabilization of MNPs.

The combination of polymer with MNPs resulted in magnetic polymer composite; it benefits from both abundant functional groups of the polymer, which endows high affinity towards dyes, and magnetic properties of MNPs. So far, such materials have been widely studied on the removal of dyes from aqueous solution, as shown in Table 3. The presence of nitrogen-containing groups in the polymers, i.e. polyethyleneimine, poly 1, 4-phenylenediamine, and polyaniline, etc., makes them

Table 3 Dye removal by magnetic polymer composites

Polymers and composites	Magnetic particles	Dye	Adsorption capacity (mg g^{-1})	pH	Temperature (°C)	References
Poly 1, 4-phenylenediamine	Fe$_3$O$_4$ nanoparticles	Direct red 81 (DR81)	144.92^a	4.0	/	[52]
Cross-linked polyethylenimine	Fe$_3$O$_4$-NH$_2$ cubic crystalline	Alizarin red S (ARS)	256.1^a	3.0	30	[51]
		Methyl orange (MO)	244.4^a	3.0	30	
		Methyl blue	172.1^a	3.0	30	
		Nuclear fast red (NFR)	138.8^a	3.0	30	
		Sunset yellow FCF (SY)	145.8^a	3.0	30	
		Alizarin green (AG)	134.6^a	3.0	30	
Chitosan/poly(vinyl alcohol) hydrogel beads	Fe$_3$O$_4$ nanoparticles	Congo red (CR)	467.3^a	/	25 ± 0.2	[22]
Oxidized multiwalled carbon nanotube (OMWCNT)- κ-carrageenan	Fe$_3$O$_4$ (10–25 nm)	Methylene blue (MB)	396.63^a	6.5	25	[5]
Poly(γ-glutamic acid) (PGA)	Fe$_3$O$_4$ (8.3 nm)	Methylene blue (MB)	78.67^a	6.0	28	[28]
Terpolymer of aniline/m-aminobenzoic acid/ m-phenylenediamine	Fe$_3$O$_4$ (39 nm)	Methylene blue (MB)	31.64^a	8.0	30	[33]
		Malachite green (MG)	29.07^a	8.0	30	

(continued)

Table 3 (continued)

Polymers and composites	Magnetic particles	Dye	Adsorption capacity (mg g^{-1})	pH	Temperature (°C)	References
Carboxymethyl chitosan-g-poly(acrylamide) (CMC-g-PAAm).	Fe_3O_4 (<3 nm)/laponite RD	Crystal violet (CV)	120[a]	/	24	[55]
Polyaniline (PANI)/mesoporous silica	Fe_3O_4 (110–130 nm)	Methyl orange (MO)	55.74[a]	4.0	0	[48]
Poly(4-styrenesulfonic acid-co-maleic acid) sodium (PSSMA)	Fe_3O_4 (∼50 nm)	Basic fuchsin (BF)	588.2[a]	7.0	25	[54]
		Crystal violet (CV)	384.6[a]	7.0	25	
		Methylene blue (MB)	270.3[a]	7.0	25	
Chitosan/carbon nanotube	Fe_3O_4 (∼65 nm)	Acid red 18 (AR18)	691.0[a]	3.0	30	[26]
Titania-polyaniline	$CoFe_2O_4$	Methyl orange (MO)	168.57[a]	/	/	[40]
Polysaccharide resin	$CuFe_2O_4$	Methylene blue (MB)	366.6[a]	8.0	/	[30]
Polyacrylamide microspheres	γ-Fe_2O_3	Methylene blue (MB)	1990[a]	8	30	[53]
		Neutral red	1937[b]	/	30	
		Gentian violet	1850[b]	/	30	

[a]Maximum adsorption capacity calculated by Langmuir isotherm model
[b]At C_0 of 100 mg/L, the equilibrium adsorption capacities for GV and NR are 1850 and 1937 mg/g

easily be positively charged in an acidic medium and in turn, facilitates the adsorption of negatively charged dyes, such as Direct red 81, and Acid Red 18 (AR18), etc., via strong electrostatic attraction, which is considered to be the dominant adsorption mechanism [48, 50–52]. The maximum adsorption capacity calculated by the Langmuir model was in the range of 55.7–256.1 mg/g at pH = 3.0 or 4.0, as shown in Table 3 [48, 51, 52]. With anionic functional groups (e.g. – COO^-, $–SO_3^-$), the polymers such as natural polysaccharides, poly(γ-glutamic acid) (PGA) and poly(4-styrenesulfonic acid-co-maleic acid) sodium (PSSMA) are highly negatively charged at pH 6.0–8.0 [5, 28, 33]; therefore, electrostatic interaction formed between polymers and cationic dyes, as shown in Fig. 7a [28]. In addition, other mechanisms, such as π–π interaction, hydrogen bonding, ion exchange and hydrophobic interaction are recommended in the adsorption process of dyes onto some magnetic polymer composites [30, 33, 39]. For example, in addition to electrostatic interactions between the functional groups ($-SO_3$, $-OH$ and $-NH$) in the polymer with the cationic dyes (MB and MG), dye was captured via π–π interactions between hydrophobic residues of dyes and aromatic cavity from the polymer backbone of magnetic polymer nanocomposite, as shown in Fig. 7b [33]. More importantly, magnetic polymer nanocomposite with porous structure or surface is believed to have extraordinary adsorption performance, i.e. a high sorption capacity as well as a fast adsorption process. For example, the porous magnetic polyacrylamide (PAM) microspheres reached an equilibrium adsorption for MB in about 200 min, and the maximum adsorption capacity calculated by Langmuir model was 1990 mg/g. Their equilibrium adsorption capacities for gentian violet (GV) and neutral (NR) at an initial concentration of 100 mg/L, were 1850 and 1937 mg/g, respectively, as shown in Table 3 [53]. The equilibrium adsorption capacity of MB onto porous magnetic PAM microspheres increased from 263 to 1977 mg/g, when initial dye concentration was changed from 5 to 300 mg/L [53].

The internal architectures of these magnetic polymer nanocomposites were examined by TEM. Two were distinguished, MNPs embedded in cross-linked polymer and core-shell structured polymer@MNPs, as shown in Fig. 8 [33, 54]. Several methods were used to fabricate magnetic polymer composites with the former structure. For example, a two-step strategy included the synthesis of MNPs
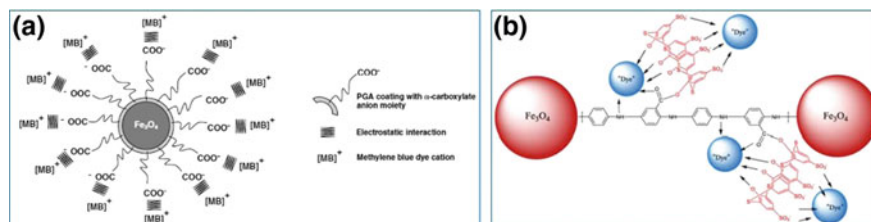

Fig. 7 Schematic diagram of proposed mechanism of **a** MB dye adsorption on PGA-MNPs (MNPs, magnetite nanoparticles; PGA, poly(γ-glutamic acid);); and **b** cationic dye adsorption on to Fe_3O_4@PAmABAmPD-TCAS nano adsorbent (PAmABAmPD, terpolymer of aniline/m-aminobenzoic acid/m-phenylenediamine; TCAS, Thiacalix(4)arene tetrasulfonate) (reprinted with permission from [28, 33])

and their dispersion in monomer-containing solution, followed by polymerization. In addition, a simple and facile one-pot solvothermal method was developed [54] and a dispersing route, in which porous PAM microspheres were dispersed in Fe(II) and Fe(III) solution and then in NaOH solution at 100 °C [53], was adopted. On the other side, core-shell structured polymer@ MNPs could be fabricated by firstly coating a dense silica and subsequently mesoporous silica, which generated pores on the surface of magnetic nanoparticles (Fe$_3$O$_4$) and allowed the PANI conjugated into the pores of mesoporous silica (MS), and finally to obtain PANI-MS@Fe$_3$O$_4$ nanocomposites [48]. Other ways to fabricate the core-shell structure were by directly coating the MNPs with a water-soluble polymer in deionized water [28], or via in situ coprecipitation method in which the synthesis started from a fine mixture of Fe(II) and Fe(III) salts and doped copolymer [33].

The reusability is considered as a key performance for investigation. The desorption of dye-loaded adsorbent was conducted by adjusting the pH of the aqueous solution since the tendency of maximum dye recovery was in general inversely proportional to the trend observed for the dye adsorption at different pHs. The adsorption of anionic dyes onto magnetic polymer composites is unfavourable at the alkaline medium, thus, NaOH or ammonium solution could be selected as effective dye desorption eluent to regenerate the spent adsorbents [51]. On the other side,
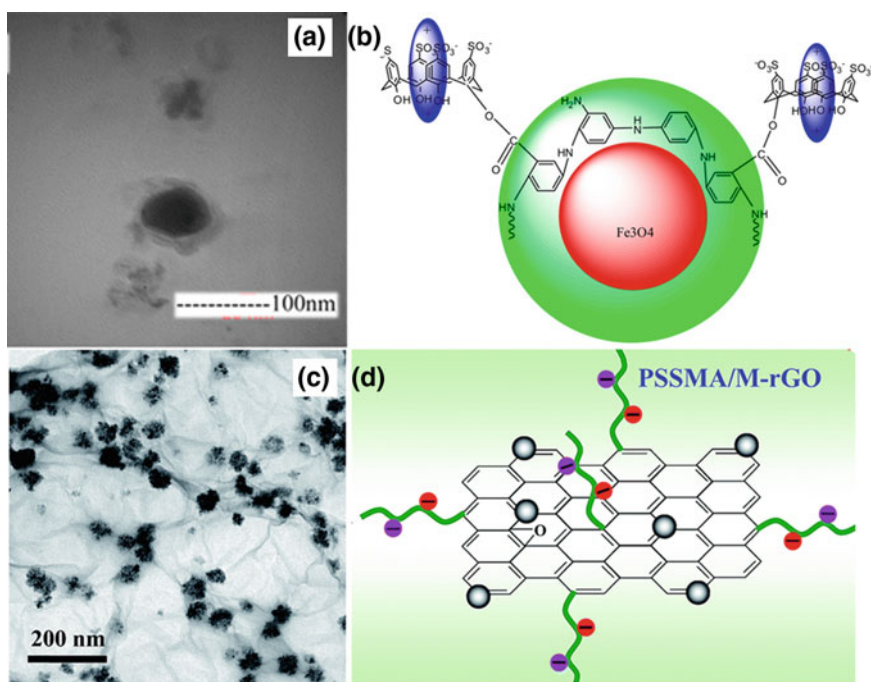
Fig. 8 TEM image and structural schematic of (**a**, **b**) Fe$_3$O$_4$@PAmABAmPD-TCAS and (**c**, **d**) poly(4-styrenesulfonic acid-co-maleic acid) sodium (PSSMA) modified magnetic reduced graphene oxide nanocomposite (PSSMA/M-rGO) (reprinted with permission from [33, 54])

desorption of cationic dyes was usually favoured in acid solution, e.g. 100–91% of the MB recovered from PGA-MNPs at pH = 1–3 [28]. The MB adsorbed onto montmorillonite/polyaniline/Fe$_3$O$_4$ (Mt/PANI/Fe$_3$O$_4$) nanocomposite could be successfully desorbed using 0.5 M HCl as the desorbing agent, and almost no decrease in the adsorption ratio was observed upon five cycles, as shown in Fig. 9a [39].

With the aid of a solvent, such as methanol or ethanol, solvent desorption technique was used to enhance the regeneration of the exhausted magnetic adsorbents [26, 48, 53]. The pH of solvent solution affected the surface charge and functional groups of adsorbent, the properties of dye molecule and in turn the desorption process [26, 48, 53]. The cationic dye MB saturated magnetic PAM microspheres could be completely regenerated (100% desorption) with acid methanol-water solution (50 v/v%, 10 mL) of pH 2 as the desorption solvent; while another cationic dye neutral red (NR) adsorbed magnetic PAM microspheres could be regenerated by neutral methanol-water solution as desorption solvent for three cycles of repeating washing process [53]. This is probably due to the difference in the charge of dye molecules, that the molecule of NR is less positively charged than MB [53]. To desorb anionic dye AR18 from the saturated magnetic chitosan-decorated carbon nanotube (mCS/CNT), which formed by compositing MNPs in chitosan-decorated carbon nanotube (CS/CNT), basic solvent solution, i.e. ammonia/ethanol (v/v, 2:3) was applied as desorption solution. The removal rate of anionic dye AR18 using regenerated mCS/CNT could be largely maintained even after 10 consecutive cycles (99.11–99.76%), indicating the excellent stability, regeneration, and reusability, as shown in Fig. 9b [26]. Such an excellent reusability might be attributed to OH$^-$ in ammonia/ethanol elution enabling the release of anionic AR18 from the adsorbent surface; the regenerated mCS/CNT adsorbent could be magnetically recycled and reused [26]. To remove anionic dye MO from polyaniline functionalized magnetic mesoporous silica composite (PANI–MS@Fe$_3$O$_4$), methanol solution containing 4% acetic acid was used as desorption eluent, in which electrostatic repulsion occurred between the protonated MO molecule and the positively charged nanocomposites adsorbent, due to the presence
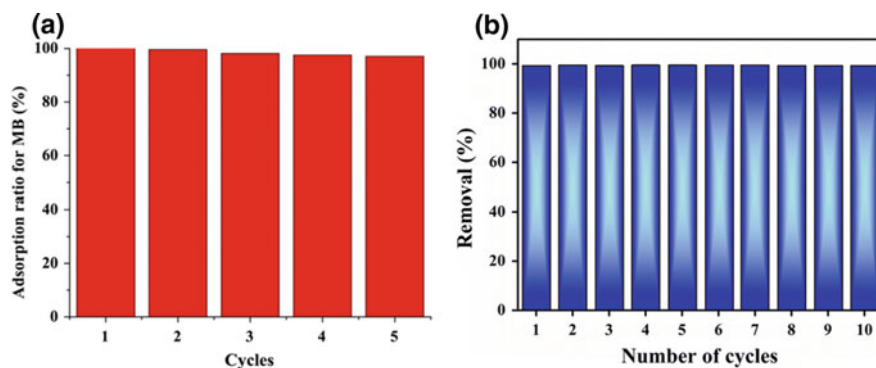

Fig. 9 **a** Adsorption cycles of MB onto Mt/PANI/Fe$_3$O$_4$ composites; **b** AR18 onto magnetic chitosan-decorated carbon nanotube (mCS/CNT) (reprinted with permission from [26, 39])

of nitrogen-containing functionalities (imine and amine groups) in PANI. Thus, there was still 80.25% of the anionic dye MO adsorbed onto the regenerated PANI–MS@Fe$_3$O$_4$ after three cycles of adsorption-desorption [48]. Other desorption solution, e.g. ethanol/water with 0.5 M KCl, was used to desorb cationic dye CV efficiently (desorption rate >97%) [55]. Taking the merit of magnetic separation, the spent magnetic polymer composites can be easily recycled and potentially reused.

5 Polymer/Clay Composites

The economic efficiency, as well as adsorption performance, are of extra importance when selecting a suitable adsorbent for practical application. Natural clays are hydrated layered aluminosilicates, which are widely available and low-cost, thus may be more viable and inexpensive for use as adsorbents to remove dyes from wastewater. Because of abundant silicon hydroxyls, negative surface charges and exchangeable cations (usually Na$^+$ and Ca^{2+}), clay minerals, e.g. attapulgite, are capable to adsorb cation dyes (e.g. MB) from water [56]. However, the relatively low adsorption capacity especially for anionic dyes due to the negatively charged surface limited their application. Organo-modification of clays with polymers is an essential way to fabricate effective adsorbents with enhanced adsorption capacity toward cationic or anionic dyes pollutants [7, 56]. Due to the presence of reactive –OH groups on their surfaces, clays can interact with reactive sites of polymers and monomers leading to the generation of polymer/clay composites [57]. In the last decades, significant research interest has been attracted on the development of polymer composites as adsorbents by incorporating inorganic clays such as attapulgite, montmorillonite, vermiculite, palygorskite and bentonite into polymeric matrices [20, 39, 57, 58]. The blending of clays not only potentially reduced fabrication cost, but also improved some properties, e.g. mechanical and thermal stability or swelling ability [20].

Among different clay minerals, bentonite is known for its good specific surface area and source abundance. The carboxymethyl cellulose (CMC) grafted by poly(2-(dimethylamino) ethyl methacrylate) modified bentonite (Bent/CMC-g-P (DMAEMA)) showed a maximum adsorption of 110.7 mg/g toward anionic MO (operation conditions: pH 6.86, 298 K and 50 min), and its removal rate was almost doubled in compared with bentonite [7]. In addition to ionic interaction, the hydrogen bonding interactions between the hydroxyl group (Si-OH, Al-OH, Fe-OH, and Mg-OH) in parent Bent and –O, –N in dye molecular greatly contributed to the observed good adsorption performance. By changing weight % of Bent in the polymer/clay composites, the surface characteristic of Bent/CMC-g-P (DMAEMA) was tuned; the resulting adsorption capacity was optimized when prepared using 20% CMC in the total amount of CMC + Bent [7]. Besides, humic acid-immobilized amine modified polyacrylamide/bentonite composite (HA-Am-PAA-B) was capable to remove cationic dyes (MG, MB, and CV) from

their single and binary component solutions, as a result of the negative surface charge of the adsorbent [59]. The carrageenan-graft-poly (acrylamide)/bentonite exhibited a maximum MB adsorption capacity up to 156.25 mg/g and its adsorption was well fitted by the Langmuir isotherm model [20].

Attapulgite (APT) and palygorskite (Pal) are another two available clays, which exist in fibrous/rod morphology [56, 58]. Featured with one-dimensional nanoscale and a large number of silanol groups, APT and Pal are good inorganic candidate materials for composite fabrication. The APT/Fe_3O_4/PANI nanocomposites showed a much higher adsorption ratio, 96.0%, for CR at pH of 7, as compared with that of APT, 14.5% (298 K, contact time: 60 min) [56]. The adsorption capacity of Reactive Red 3BS onto the polyamidoamine (PAMAM) dendrimer-functionalized Pal adsorbents markedly increased from 34.2 to 322.6 mg/g (293 K, contact time: 20 min) by increasing addition of PAMAM, which contains amino-terminated groups. The anionic dyes could be trapped and then stabilized in the cavities of PAMAM dendrimers due to the host-guest affinity [58].

Temperature is one of the factors affecting equilibrium capacity of adsorbents, which correlates with the exothermicity or endothermicity nature of adsorption. Mostly, the adsorption capacity increased by increasing of temperature during the endothermic adsorption of dyes onto polymer/clay composites, which could be confirmed by the positive values of enthalpy change ($\Delta H°$) [57, 60]. The diffusion rate of dye molecules from solution to the adsorbent surface was also enhanced with increasing temperature, thus, adsorption capacity was improved [20, 57]. In the case of MO adsorption onto 20CMC-Bent (20% of CMC in the total amount of CMC + Bent composite), the negative $\Delta H°$ value indicated an exothermic adsorption process [7].

The adsorption capacity of cationic dye onto polymer/clay composites was observed to increase at higher pH [20, 57]; this was explained by the stronger electrostatic attraction formed between deprotonated functional groups of the adsorbents and positively-charged dye molecules. The maximum removal rate % of MG, MB, and CV onto the HA-Am-PAA-B was 99.7, 99.3, and 98.8%, respectively, at pH 6.0 with an initial dye concentration of 200 μmol/L [59]. The optimized adsorption pH was observed in the range of 6.0–8.0, under which the carboxylic and phenolic groups were deprotonated and the surface charge of adsorbent was negative (pH_{pzc} 4.8) [59].

Interestingly, at pH = 6.3, the Mt/PANI/Fe_3O_4 composite, which was protonated via treating with 0.1 M HCl, displayed a maximum adsorption ratio of 98.1% toward anionic dye CR; whilst the dedoped Mt/PANI/Fe_3O_4 showed excellent adsorption ratio of 99.6 and 96.2% to cationic dyes MB and Brilliant green (BG), respectively (298 K, contact time: 60 min) [39]. This difference resulted from the variation on the surface charge, that the dedoped Mt/PANI/Fe_3O_4 was negatively charged, as compared to positively charged Mt/PANI/Fe_3O_4 after acid treatment. The resulting clay/polymer composite showed excellent adsorption capacity to both cationic dyes and anionic dyes, in relative to the original Mt adsorbent [39]. Moreover, by introducing magnetic particles, such as Fe_3O_4 and $CoFe_2O_4$, the clay/polymer composites were able to be recovered by magnetic separation for reuse [39, 56, 60]. For example, via magnetic separation, no decrease in the adsorption ratio of

MB onto the dedoped Mt/PANI/Fe$_3$O$_4$ composite was observed upon five successive cycles [39].

6 Polymer/by-Products or Waste Composites

Recently, there has been increasing research interest in exploring polymer composites synthesized with industrial or agricultural by-products or waste, such as coir pith, fly ash, flax shrive, sawdust, sugarcane molasses, and almond shell waste, etc., due to the biodegradability, low cost and great availability [2, 3, 61–65]. By-products or waste materials may have a certain affinity to cationic dyes, because of the presence of surface hydroxyl groups; however, the adsorption capacity of anionic dyes was usually found to be low [63]. For example, the use of flax shrive cellulose exhibited only ~ 0.5 mg/g adsorption towards RR228 [3]; whilst that of almond shell waste (AS) to acid blue 25 (AB25) was less than 2.4 mg/g [63]. Benefited from functional groups of polymers, their incorporated polymer composites exhibited enhanced dye adsorption capacity.

In order to achieve good adsorption property, the physical or chemical modification is usually adopted to increase surface groups of waste/by-products for functionalization with polymers and in turn improve their adhesion with the polymer matrix. For example, after heat and alkali treatment, the surface area of coal fly ash (CFA), a coal combustion by-product, increased from 66.78 to 102.89 m^2/g, accompanied with greater total pore volume and average pore size; these features were believed to contribute in enhancing adsorption capacity. Moreover, the modified CFA possessed a greater amount of surface silanol groups (Si–OH), which could be functionalized with polyethyleneimine (PEI) to fabricate composite adsorbents. Thanks to the amine group at the end of the PEI chain as well as the high amine density, the Langmuir maximum adsorption capacity of CFA/PEI composite was found to be 316.75 mg/g for reactive red 2 (RR2) (pH = 3, 313 K) and 174.83 mg/g for MG (pH = 8, 308 K), respectively [61]. Goes and co-workers chemically modified cellulose with 4,4′-diphenylmethane diisocyanate (MDI); the resulting material showed enhanced adsorption capacity [2]. The equilibrium adsorption capacities of MB onto polyurethane foams with unmodified cellulose was 1.57 mg/g; that on polyurethane with chemically modified cellulose increased to 1.83 mg/g under the same operating conditions. This difference might result from the structural changes caused by the reaction of MDI on cellulose surface [2].

7 Conclusions

Adsorption has been investigated as an effective approach for the treatment of dye-containing wastewater. Polymers and polymer composites exhibited attractive features of high strength, good flexibility, and ease of modification or

functionalization, thus as potential adsorbents with high adsorption capacity, fast adsorption rate and good reusability. Recent advances in polymers and polymer composites, such as PANI composites, magnetic polymer composites, polymer/clay composites and polymer/by-products or waste composites, were reviewed in terms of their properties and adsorption. The regeneration of spent polymers and polymer composites and subsequent reuse was also discussed, which potentially improved the cost efficiency of adsorbents.

Both the properties of adsorbents and dyes were considered as the key factors tuning adsorptive dye removal from aqueous solution. Generally, polymers and polymer composites attract the dye molecules via electrostatic interaction, van der Waals forces, π–π interaction, and hydrogen bonding. Electrostatic interaction and hydrogen bonding are two of the most commonly underlying mechanisms governing the sorption process, which were found to be affected by the complex physicochemical natures of dyes (e.g. cationic, anionic and nonionic dyes) and the properties of adsorbents (such as surface acidity or charge, zeta potential, pore size and its distribution, and surface area). The polymer sorbents with enhanced positively charged surface sites via modification or functionalization were found to favour the removal of anionic dyes and vice versa. By combining with inorganic materials, e.g. graphene, the resulting polymer composites exhibited a broad-spectrum adsorption performance, which was explained by the π–π interactions between aromatic or heterocyclic structures of dyes and graphene sheets.

Polymers and polymer composites with special characteristics, such as the presence of an internal hydrophobic cavity, in the forms of nanosized particles or 1D nanofibers, and the introduction of 3D porous structure (i.e. nanopores or mesopores), could facilitate the adsorption. The selectivity during adsorption could be achieved via tuning the pore size in the porous polymers or polymer composites, which was suggested as being governed by the size-selective mechanism.
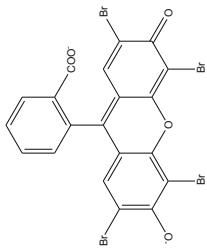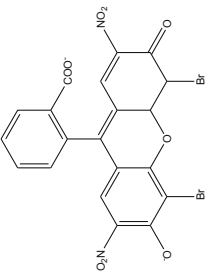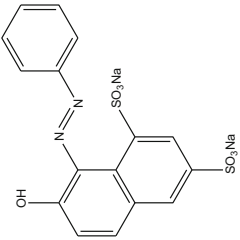
Note that the adsorption performance was significantly affected by a number of operating conditions, including solution pH, temperature, initial dye concentration, and equilibrium time. For example, the solution pH would vary both solution chemistry and surface binding sites of adsorbents. Therefore, it is necessary for optimization of operation conditions towards enhanced adsorptive dye removal from water.
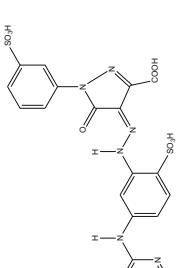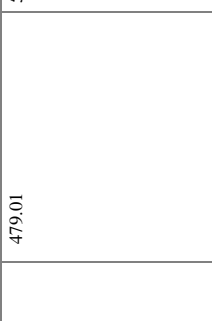
Appendix

See Table 4.

Table 4 Molecular structure/weight, abbreviation, species and λ_{max} of dyes in reports

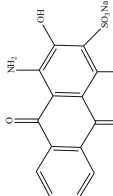| Dye	Abbreviation	Molecular weight (g mol⁻¹)	λ_{max} (nm)	Ionic species	Molecular structure	References
Eosin yellow	EY	645.89	517	Anionic		[42]
Eosin blue	EB	578.09	516	Anionic		[42]
Orange G	OG	452.37	480	Anionic		[42]
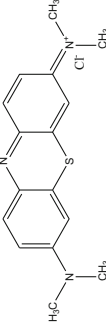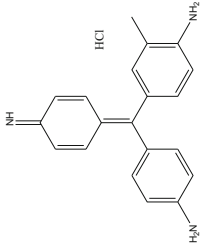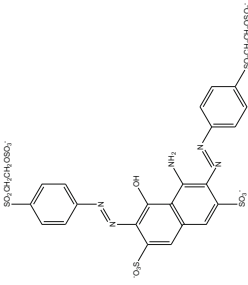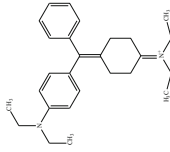
(continued)

Table 4 (continued)

Dye	Abbreviation	Molecular weight (g mol^{-1})	λ_{max} (nm)	Ionic species	Molecular structure	References
Reactive orange-14	RO	631.383	420	Anionic		[42]
OrangeII (C l Acid orange 7)	/	350.32	483	Anionic	 Cl Acid Orange 7	[31, 42]
Rhodammine B	RHB	479.01	554	Cationic		[42]

(continued)

Table 4 (continued)

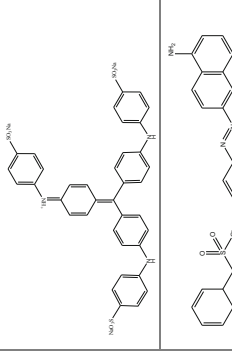| Dye	Abbreviation	Molecular weight (g mol^{-1})	λ_{max} (nm)	Ionic species	Molecular structure	References
Methylene blue	MB	373.9	663	Cationic		[28]
Basic violet 14	BV	337.85	545	Cationic		[17]
Reactive black 5	RB5	991.82	597	Anionic		[14]
Brilliant green	BG	482.63	625	Cationic		[45]
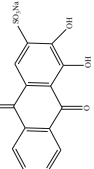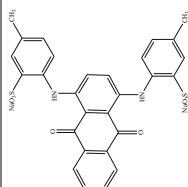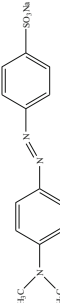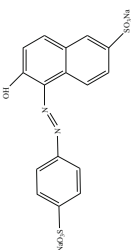
(continued)

Table 4 (continued)

Dye	Abbreviation	Molecular weight (g mol^{-1})	λ_{max} (nm)	Ionic species	Molecular structure	References
Reactive red 194	RR-194	984.2062	542	Anionic		[8]
Direct blue 199	DB-199	775.21	608	Anionic		[8]
Acid blue 62	AB-62	400.45	620	Anionic	Acid Blue 62	[8]
CI Acid red 88	AR 88	400.38	505	Anionic		[31]
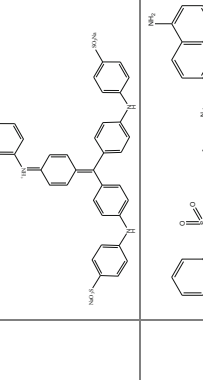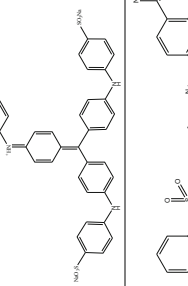
Table 4 (continued)

Dye	Abbreviation	Molecular weight (g mol^{-1})	λ_{max} (nm)	Ionic species	Molecular structure	References
Alizarin red S	ARS	342.26	423	Anionic		[51]
Nuclear fast red	NFR	357.28	518	Anionic		[51]
Alizarin green	AG	622.58	642	Anionic		[51]
Methyl orange	MO	327.33	463	Anionic		[51]
Sunset yellow FCF	SY	452.37	482	Anionic		[51]
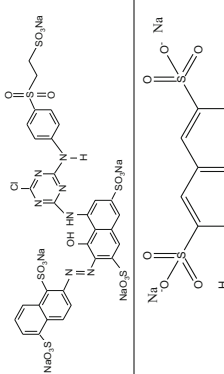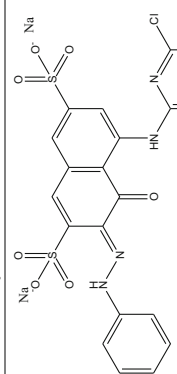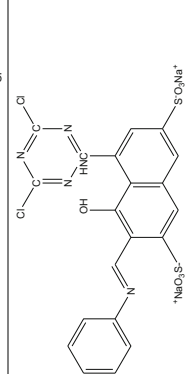
(continued)

Table 4 (continued)

Dye	Abbreviation	Molecular weight (g mol^{-1})	λ_{max} (nm)	Ionic species	Molecular structure	References
Methyl blue	/	799.80	600	Anionic		[51]
Congo red	CR	696.68	497/500	Anionic		[14, 34]
Malachite green	MG	364.92	617	Cationic		[41]
Acid red 18	AR18	604.47	507	Anionic		[26, 65]
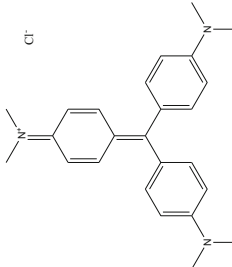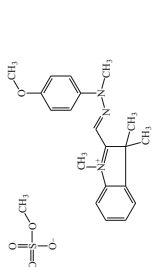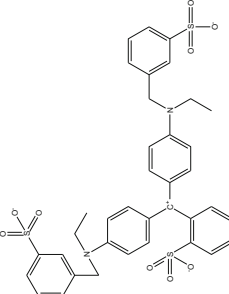
(continued)

Table 4 (continued)

Dye	Abbreviation	Molecular weight (g mol^{-1})	Molecular structure	Ionic species	λ_{max} (nm)	References
Reactive red 3BS (C.I. reactive red 195)	/	1118.83		Anionic	546	[58]
Reactive red	RR	613.92		Anionic	547	[25]
Active brilliant red X-3B	/	615.33		Anionic	540.5	[27]

(continued)

Table 4 (continued)

Dye	Abbreviation	Molecular weight (g mol^{-1})	λ_{max} (nm)	Ionic species	Molecular structure	References
Crystal violet (methyl violet 10B)	CV	407.99	595	Cationic		[55]
Basic yellow 28	BY28	433.52	420	Cationic		[25]
Brilliant blue 133	BB133	792.85	609.5	Anionic		[25]

References

1. Ngulube T et al (2017) An update on synthetic dyes adsorption onto clay based minerals: a state-of-art review. J Environ Manag 191:35–57
2. Goes MM et al (2016) Polyurethane foams synthesized from cellulose-based wastes: kinetics studies of dye adsorption. Ind Crops Prod 85:149–158
3. Wang L, Li J (2013) Adsorption of C.I. reactive red 228 dye from aqueous solution by modified cellulose from flax shive: kinetics, equilibrium, and thermodynamics. Ind Crops Prod 42(Supplement C):153–158
4. Kanmani P et al (2017) Environmental applications of chitosan and cellulosic biopolymers: a comprehensive outlook. Bioresour Technol 242:295–303
5. Duman O et al (2016) Synthesis of magnetic oxidized multiwalled carbon nanotube-kappa-carrageenan-Fe_3O_4 nanocomposite adsorbent and its application in cationic methylene blue dye adsorption. Carbohydr Polym 147:79–88
6. Rajabi M, Mahanpoor K, Moradi O (2017) Removal of dye molecules from aqueous solution by carbon nanotubes and carbon nanotube functional groups: critical review. Rsc Adv 7(74):47083–47090
7. Li W et al (2017) Tunable adsorption properties of bentonite/carboxymethyl cellulose-g-poly (2-(dimethylamino) ethyl methacrylate) composites toward anionic dyes. Chem Eng Res Des 124:260–270
8. Javadian H, Angaji MT, Naushad M (2014) Synthesis and characterization of polyaniline/gamma-alumina nanocomposite: a comparative study for the adsorption of three different anionic dyes. J Ind Eng Chem 20(5):3890–3900
9. Ezzatahmadi N et al (2017) Clay-supported nanoscale zero-valent iron composite materials for the remediation of contaminated aqueous solutions: a review. Chem Eng J 312:336–350
10. Pandey S (2017) A comprehensive review on recent developments in bentonite-based materials used as adsorbents for wastewater treatment. J Mol Liq 241:1091–1113
11. Sulyman M, Namiesnik J, Gierak A (2017) Low-cost adsorbents derived from agricultural by-products/wastes for enhancing contaminant uptakes from wastewater: a review. Polish J Environ Stud 26(2):479–510
12. Xiao J et al (2017) Multifunctional graphene/poly(vinyl alcohol) aerogels: in situ hydrothermal preparation and applications in broad-spectrum adsorption for dyes and oils. Carbon 123:354–363
13. Voisin H et al (2017) Nanocellulose-based materials for water purification. Nanomaterials 7(3):19
14. Qiu Y, Ling F (2006) Role of surface functionality in the adsorption of anionic dyes on modified polymeric sorbents. Chemosphere 64(6):963–971
15. Zhang L et al (2012) Facile and large-scale synthesis of functional poly(m-phenylenediamine) nanoparticles by Cu2 + -assisted method with superior ability for dye adsorption. J Mater Chem 22(35):18244–18251
16. Gezici O et al (2016) Humic-makeup approach for simultaneous functionalization of polyacrylonitrile nanofibers during electrospinning process, and dye adsorption study. Soft Mater 14(4):278–287
17. Elkady MF, El-Aassar MR, Hassan HS (2016) Adsorption profile of basic dye onto novel fabricated carboxylated functionalized co-polymer nanofibers. Polymers 8(5):177
18. Chauque EFC et al (2017) Electrospun polyacrylonitrile nanofibers functionalized with EDTA for adsorption of ionic dyes. Phys Chem Earth 100:201–211
19. Almasian A, Olya ME, Mahmoodi NM (2015) Preparation and adsorption behavior of diethylenetriamine/polyacrylonitrile composite nanofibers for a direct dye removal. Fibers Polym 16(9):1925–1934
20. Pourjavadi A et al (2016) Porous Carrageenan-g-polyacrylamide/bentonite superabsorbent composites: swelling and dye adsorption behavior. J Polym Res **23**(3)

21. Ekici S, Isikver Y, Saraydin D (2006) Poly(acrylamide-sepiolite) composite hydrogels: preparation, swelling and dye adsorption properties. Polym Bull 57(2):231–241
22. Zhu HY et al (2012) Novel magnetic chitosan/poly(vinyl alcohol) hydrogel beads: preparation, characterization and application for adsorption of dye from aqueous solution. Bioresour Technol 105:24–30
23. Zhu L et al (2017) Adsorption of dyes onto sodium alginate graft poly(acrylic acid-co-2-acrylamide-2-methyl propane sulfonic acid)/kaolin hydrogel composite. Polym Polymer Compos 25(8):627–634
24. Das S et al (2017) Folic acid-polyaniline hybrid hydrogel for adsorption/reduction of chromium(VI) and selective adsorption of anionic dye from water. Acs Sustain Chem Eng 5(10):9325–9337
25. Zhu W et al (2016) Functionalization of cellulose with hyperbranched polyethylenimine for selective dye adsorption and separation. Cellulose 23(6):3785–3797
26. Wang S et al (2014) Highly efficient removal of acid Red 18 from aqueous solution by magnetically retrievable Chitosan/carbon nanotube: batch study, isotherms, kinetics, and thermodynamics. J Chem Eng Data 59(1):39–51
27. Deng H, Wei Z, Wang X (2017) Enhanced adsorption of active brilliant red X-3B dye on chitosan molecularly imprinted polymer functionalized with Ti(IV) as Lewis acid. Carbohydr Polym 157:1190–1197
28. Inbaraj BS, Chen BH (2011) Dye adsorption characteristics of magnetite nanoparticles coated with a biopolymer poly(gamma-glutamic acid). Bioresour Technol 102(19):8868–8876
29. Wang L, Li Q (2010) Wang A Adsorption of cationic dye on N,O-carboxymethyl-chitosan from aqueous solutions: equilibrium, kinetics, and adsorption mechanism. Polym Bull 65(9):961–975
30. Beyki MH et al (2017) Clean approach to synthesis of graphene like CuFe2O4@polysaccharide resin nanohybrid: bifunctional compound for dye adsorption and bacterial capturing. Carbohydr Polym 174:128–136
31. Shimizu Y, Saito Y, Nakamura T (2006) Crosslinking of chitosan with a trifunctional crosslinker and the adsorption of acid dyes and metal ions onto the resulting polymer. Adsorpt Sci Technol 24(1):29–39
32. Zhang X et al (2015) Adsorption of basic dyes on beta-cyclodextrin functionalized poly (styrene-alt-maleic anhydride). Sep Sci Technol 50(7):947–957
33. Lakouraj MM, Norouzian R-S, Balo S (2015) Preparation and cationic dye adsorption of novel Fe$_3$O$_4$ supermagnetic/thiacalix 4 arene tetrasulfonate self-doped/polyaniline nanocomposite: kinetics, isotherms, and thermodynamic study. J Chem Eng Data 60(8):2262–2272
34. Liu H, Liu H (2017) Selective dye adsorption and metal ion detection using multifunctional silsesquioxane-based tetraphenylethene-linked nanoporous polymers. J Mater Chem A 5(19):9156–9162
35. Liu J et al (2017) Preparation of polyhedral oligomeric silsesquioxane based cross-linked inorganic-organic nanohybrid as adsorbent for selective removal of acidic dyes from aqueous solution. J Coll Interf Sci 497:402–412
36. Zhao W et al (2015) Functionalized graphene sheets with poly(ionic liquid)s and high adsorption capacity of anionic dyes. Appl Surf Sci 326:276–284
37. Agarwal S et al (2016) Synthesis and characteristics of polyaniline/zirconium oxide conductive nanocomposite for dye adsorption application. J Mol Liq 218:494–498
38. Wang L et al (2012) Stable organic-inorganic hybrid of polyaniline/α-zirconium phosphate for efficient removal of organic pollutants in water environment. ACS Appl Mater Interf 4(5):2686–2692
39. Mu B et al (2016) Preparation, characterization and application on dye adsorption of a well-defined two-dimensional superparamagnetic clay/polyaniline/Fe3O4 nanocomposite. Appl Clay Sci 132:7–16
40. Xiong P et al (2013) Ternary titania-cobalt ferrite-polyaniline nanocomposite: a magnetically recyclable hybrid for adsorption and photodegradation of dyes under visible light. Ind Eng Chem Res 52(30):10105–10113

41. Zeng Y et al (2013) Enhanced adsorption of malachite green onto carbon nanotube/polyaniline composites. J Appl Polym Sci 127(4):2475–2482
42. Majumdar S, Saikia U, Mahanta D (2015) Polyaniline-coated filter papers: cost effective hybrid materials for adsorption of dyes. J Chem Eng Data 60(11):3382–3391
43. Pandiselvi K, Manikumar A, Thambidurai S (2014) Synthesis of novel polyaniline/MgO composite for enhanced adsorption of reactive dye. J Appl Polym Sci 131(9)
44. Saad M et al (2017) Synthesis of polyaniline nanoparticles and their application for the removal of crystal violet dye by ultrasonicated adsorption process based on response surface methodology. Ultrason Sonochem 34:600–608
45. Salem MA, Elsharkawy RG, Hablas MF (2016) Adsorption of brilliant green dye by polyaniline/silver nanocomposite: kinetic, equilibrium, and thermodynamic studies. Eur Polym J 75:577–590
46. Pandiselvi K, Thambidurai S (2016) Synthesis of adsorption cum photocatalytic nature of polyaniline-ZnO/chitosan composite for removal of textile dyes. Desalin Water Treat 57(18):8343–8357
47. Bingol D et al (2012) Analysis of adsorption of reactive azo dye onto $CuCl_2$ doped polyaniline using Box-Behnken design approach. Synth Metals 162(17–18):1566–1571
48. Mahto TK et al (2015) Kinetic and thermodynamic study of polyaniline functionalized magnetic mesoporous silica for magnetic field guided dye adsorption. Rsc Adv 5(59):47909–47919
49. Anuradha Jabasingh S, Ravi T, Yimam A (2017) Magnetic hetero-structures as prospective sorbents to aid arsenic elimination from life water streams. Water Sci
50. Zhou L, He B, Huang J (2013) One-step synthesis of robust amine- and vinyl-capped magnetic iron oxide nanoparticles for polymer grafting, dye adsorption, and catalysis. Acs Appl Mater Interf 5(17):8678–8685
51. Chen B et al (2016) Magnetically recoverable cross-linked polyethylenimine as a novel adsorbent for removal of anionic dyes with different structures from aqueous solution. J Taiwan Inst Chem Eng 67:191–201
52. Beyki MH et al (2016) Green synthesized Fe_3O_4 nanoparticles as a magnetic core to prepare poly 1, 4 phenylenediamine nanocomposite: employment for fast adsorption of lead ions and azo dye. Desalin Water Treat 57(59):28875–28886
53. Yao T et al (2015) Investigation on efficient adsorption of cationic dyes on porous magnetic polyacrylamide microspheres. J Hazard Mater 292:90–97
54. Song Y-B et al (2015) Poly(4-styrenesulfonic acid-co-maleic acid)-sodium-modified magnetic reduced graphene oxide for enhanced adsorption performance toward cationic dyes. Rsc Adv 5(106):87030–87042
55. Mahdavinia GR, Karami S (2015) Synthesis of magnetic carboxymethyl chitosan-g-poly (acrylamide)/laponite RD nanocomposites with enhanced dye adsorption capacity. Polym Bull 72(9):2241–2262
56. Mu B, Wang A (2015) One-pot fabrication of multifunctional superparamagnetic attapulgite/Fe_3O_4/polyaniline nanocomposites served as an adsorbent and catalyst support. J Mater Chem A 3(1):281–289
57. Dong K et al (2013) Polyurethane-attapulgite porous material: preparation, characterization, and application for dye adsorption. J Appl Polym Sci 129(4):1697–1706
58. Zhou S et al (2015) Novel polyamidoamine dendrimer-functionalized palygorskite adsorbents with high adsorption capacity for Pb^{2+} and reactive dyes. Appl Clay Sci 107:220–229
59. Anirudhan TS, Suchithra PS (2009) Adsorption characteristics of humic acid-immobilized amine modified polyacrylamide/bentonite composite for cationic dyes in aqueous solutions. J Environ Sci 21(7):884–891
60. Ai L, Zhou Y, Jiang J (2011) Removal of methylene blue from aqueous solution by montmorillonite/$CoFe_2O_4$ composite with magnetic separation performance. Desalination 266(1):72–77

61. Dash S et al (2016) Fabrication of inexpensive polyethylenimine-functionalized fly ash for highly enhanced adsorption of both cationic and anionic toxic dyes from water. Energy Fuels 30(8):6646–6653
62. Gonte RR, Shelar G, Balasubramanian K (2014) Polymer-agro-waste composites for removal of Congo red dye from wastewater: adsorption isotherms and kinetics. Desalin Water Treat 52(40–42):7797–7811
63. Jabli M et al (2017) Almond shell waste (Prunus dulcis): Functionalization with dimethy-diallyl-ammonium-chloride-diallylamin-co-polymer and chitosan polymer and its investigation in dye adsorption. J Mol Liq 240:35–44
64. Namasivayam C, Sureshkumar MV (2006) Anionic dye adsorption characteristics of surfactant-modified coir pith, a 'waste' lignocellulosic polymer. J Appl Polym Sci 100(2):1538–1546
65. Shabandokht M, Binaeian E, Tayebi H-A (2016) Adsorption of food dye acid red 18 onto polyaniline-modified rice husk composite: isotherm and kinetic analysis. Desalin Water Treat 57(57):27638–27650
66. Lu Y-S et al (2016) Direct assembly of mesoporous silica functionalized with polypeptides for efficient dye adsorption. Chem-a Eur J 22(3):1159–1164